

Electronic Supplementary Information

Neutral nickel complexes with tetradentate *N*-heterocyclic carbene amidate ligands for electrocatalytic hydrogen evolution

Si Si,^a Wenxun Song,^a Jie Chen,^{*a} Weimin Zhang,^a Wenhua Ji,^c Wonwoo
Nam,^{*b} and Bin Wang^{*a}

^a *School of Chemistry and Chemical Engineering, University of Jinan, Jinan 250022,
Shandong Province, China.*

^b *Department of Chemistry and Nano Science, Ewha Womans University, Seoul 03760,
Korea.*

^c *Key Laboratory for Applied Technology of Sophisticated Analytical Instruments of
Shandong Province, Shandong Analysis and Test Center, Qilu University of Technology
(Shandong Academy of Sciences), Jinan 250014, China.*

*To whom correspondence should be addressed.

chm_chenj@ujn.edu.cn

wwnam@ewha.ac.kr

chm_wangb@ujn.edu.cn

Table of Contents

Experimental Section	S3
Electrochemical Measurements	S4
Calculation Methods of TOFs from Electrochemical Data	S5
Determination of Overpotential with TFA in CH ₃ CN	S6
Calculation Methods of Faraday Efficiency (FE).....	S7
General Procedure for Ligand Synthesis	S8
Synthesis and Characterization of Nickel(II) Complexes.....	S12
References.....	S15
Table S1	S16
Table S2	S17
Table S3	S18
Table S4	S19
Fig. S1.....	S21
Fig. S2.....	S22
Fig. S3.....	S23
Fig. S4.....	S24
Fig. S5.....	S25
Fig. S6.....	S26
Fig. S7.....	S27
Fig. S8.....	S28
Additional Data: ¹ H and ¹³ C NMR Spectra	S29

Experimental Section

Materials. Chemicals were purchased from commercial sources. Organic solvents used were analytical grade. Solvents were dried according to published procedures and distilled under argon prior to use.

Apparatuses. NMR spectra were recorded on Bruker Avance III 400 (400 MHz for ^1H ; 100 MHz for ^{13}C) or Bruker Avance III 600 (600 MHz for ^1H ; 150 MHz for ^{13}C). For X-ray structural analysis, crystallographic data collections were carried out on a Bruker SMART AXS diffractometer equipped with a monochromator in the Mo $\text{K}\alpha$ ($\lambda = 0.71073 \text{ \AA}$) incident beam. Gas analysis for bulk electrolysis experiments were performed using 50 μL sample injections on a Beifen 6890A series gas chromatograph. Gas sample H_2 was analyzed using thermal conductivity detector (TCD), stainless-steel column packed with molecular sieves ($5 \text{ \AA} \times 3 \text{ m}$), and Ar as the carrier gas (flow rate = 30 mL min^{-1}). Aliquots (50 μL) of the gas headspace were injected into the GC every time to analyze the gas products formed.

Electrochemical Measurements

Electrochemical data were carried out in CHI-630E potentiostat instrument. Solution (total 5.0 mL) of the catalyst (1.0 mM) was placed in an undivided cell. Glassy carbon (GC, 3.0 mm of diameter) electrode was used as working electrode, Ag/AgCl with saturated KCl solution as reference electrode and Pt wire as counter electrode. Before each measurement, working electrode was polished with 0.05 μm alumina paste and rinsed with HNO_3 , acetone, ethanol, and water, respectively. All redox potentials in the present work are reported versus Fc/Fc^+ . Tetrabutylammonium hexafluorophosphate ($n\text{-Bu}_4\text{NPF}_6$) (0.10 M) was used as a supporting electrolyte in dry CH_3CN . All the electrochemical reactions were conducted under N_2 atmosphere. Controlled potential electrolysis (CPE) experiment was conducted in a 10 mL Schlenk tube. Glassy carbon (GC, 3.0 mm of diameter) electrode was used as working electrode, Ag/AgCl with saturated KCl solution as reference electrode and Pt wire as counter electrode. 5.0 mL samples were prepared as 1.0 mM catalyst, 0.1 M $n\text{-Bu}_4\text{NPF}_6$, and 0.2 M trifluoroacetic acid. Before each measurement, the electrolyte was conducted under N_2 atmosphere for 30 min. CPE was operated for 3 hours. Applied potential was -1.6 V vs Fc/Fc^+ . Gas analysis for CPE was performed using 1 mL sample aliquots taken from the headspace of the electrochemical cell and injected on GC equipment. The faradaic efficiency of each experiment was determined by dividing the measured amount of H_2 by passed charge during CPE.

Calculation Methods of TOFs from Electrochemical Data

TOFs were calculated by using cyclic voltammograms. In cyclic voltammograms at a certain concentration of acid, the catalytic current is proportional to the concentration of catalyst([cat]), acid concentration ([Q]^y), diffusion coefficient (D), electrode surface area (A), and rate constant of catalytic reaction (*k*_{cat}) (eq S1). If the concentration of catalyst is sufficiently smaller than acid, the catalytic reaction can be assumed as pseudo-first-reaction for acid (y = 1). The rate of catalytic reaction can be obtained by squaring (*i*_{cat}/*i*_p) and arranging the equation for *k*_{cat}[Q]. *i*_p can be illustrated by the Randles-Sevcik equation (eq S2) and dividing *i*_{cat} by *i*_p can cancel out electrode surface area (A) and diffusion coefficient (D) (eq S3). Equation 3 can be described easier by calculating constant as shown in eq S4.

$$i_{cat} = n_{cat}FA[cat]\sqrt{Dk_{cat}[Q]^y} \quad (\text{eq S1})$$

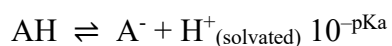
$$i_p = 0.446n_pFA[cat]\sqrt{\frac{n_pFvD}{RT}} \quad (\text{eq S2})$$

$$\text{Rate of catalytic reaction (TOF, s}^{-1}\text{)} = k_{cat}[Q] = \frac{Fvn_p^3}{RT} \left(\frac{0.4463}{n_{cat}}\right)^2 \left(\frac{i_{cat}}{i_p}\right)^2 \quad (\text{eq S3})$$

$$\text{TOF} = k_{cat}[Q] = 1.94 v \left(\frac{i_{cat}}{i_p}\right)^2 \quad (\text{eq S4})$$

Determination of Overpotential with TFA in CH₃CN

The determination of overpotential from cyclic voltammograms includes taking the potential value at a specific dot on these curves and weighing up it to the corresponding theoretical points for an electrochemically reversible process. Since the pK_a ($pK_a^{\text{MeCN}} = 12.7$) and the standard redox potential of TFA in MeCN ($E_{\text{H}^+/\text{H}_2}^\circ = -0.07$ V) are reported^{S1,S2}, the equilibrium potential ($E_{\text{AH}/\text{H}_2, \text{A}^-}^\circ = -0.82$ V) can be calculated according to eq S5 using Evans' expression^{S3}. The well-defined potential on voltammograms corresponding the half the maximum current of catalytic current is $E_{\text{cat}/2}$. This value can be read straightly on experimental GC voltammograms. The overpotential of the electrocatalytic proton reduction catalyzed by nickel complex was measured using eq S6.



$$E_{\text{AH}}^\circ = E_{\text{H}^+/\text{H}_2}^\circ - \frac{2.303RT}{F} pK_a \text{ (eq S5)}$$

$$\text{Overpotential} = |E_{\text{AH}}^\circ - E_{\text{cat}/2}| \text{ (eq S6)}$$

Calculation Methods of Faraday Efficiency (FE)

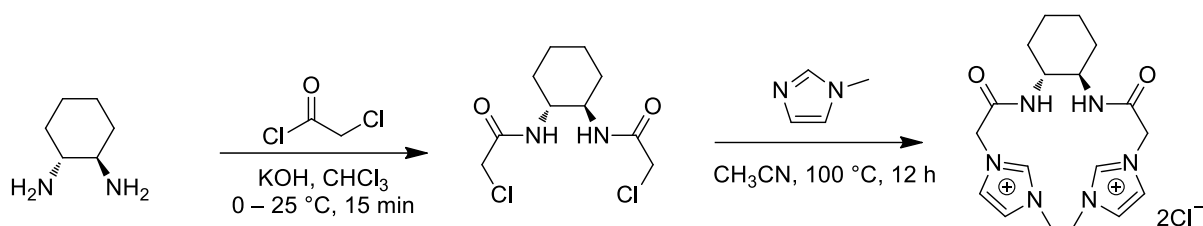
Generally, FE is determined by the equation

$$FE = n(\text{H}_2)/(Q/2F) = 2Fn(\text{H}_2)/Q \text{ (eq S7)}$$

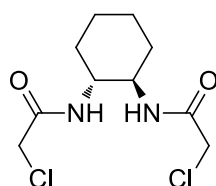
During the constant potential electrolysis (CPE) of **3**, total charge consumed was 34.8 C in 3 hours and 1.15×10^{-4} mol H_2 gas was collected in a home-made set up.

$$\text{Therefore, Faraday efficiency (FE)} = (2 \times 96485 \times 115 \times 10^{-6})/34.8 = 63.8\%$$

General Procedure for Ligand Synthesis



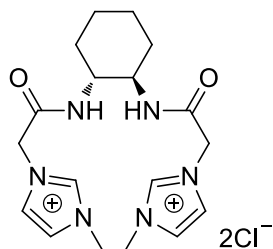
N,N'-(((1*R*,2*R*)-Cyclohexane-1,2-diyl)bis(2-chloroacetamide))



(1*R*,2*R*)-1,2-cyclohexanediamine (2.28 g, 20 mmol) was dissolved in CHCl₃ (50 mL), and KOH (2.25 g, 40 mmol) in H₂O (20 mL) was added. Then, chloroacetyl chloride (4.52 g, 40 mmol) in CHCl₃ (50 mL) was added drop wise to the mixture with stirring at 0 °C. After 15 minutes, the solid was filtered and washed with Et₂O (20 mL). Drying in *vacuo* yielded a solid (4.54 g, 17 mmol, 85%). The characterization data was identical to that reported in the literature.^{S4}

¹H NMR (600 MHz, CDCl₃): δ 6.83 (s, 2H), 3.99 (d, *J* = 6.0 Hz, 4H), 3.75 (s, 2H), 2.07 (d, *J* = 6.0 Hz, 2H), 1.80 (dd, *J* = 24.0, 16.0 Hz, 2H), 1.34 (d, *J* = 6.0 Hz, 4H).

3,3'-(((1*R*,2*R*)-Cyclohexane-1,2-diylbis(azanediyl))bis(2-oxoethane-2,1-diyl))bis(1-methyl-1H-imidazol-3-ium)



A solution of *N,N'*-(((1*R*,2*R*)-cyclohexane-1,2-diyl)bis(2-chloroacetamide)) (6.89 g, 25.8 mmol) and 1-methylimidazole (4.23 g, 51.5 mmol) in acetonitrile was refluxed at 100 °C for 12 h. The mixture was filtered, and the solvent was removed under reduced pressure, the product was

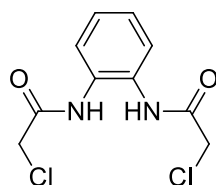
obtained as a solid (6.23 g, 14.4 mmol, 56%).

¹H NMR (400 MHz, DMSO-*d*₆): δ 9.50 – 9.30 (m, 2H), 8.59 – 8.43 (m, 2H), 7.87 – 7.78 (m, 2H), 7.76 – 7.68 (m, 2H), 5.26 – 5.13 (m, 2H), 4.97 (d, *J* = 17.0 Hz, 2H), 3.91 (s, 6H), 3.61 – 3.50 (m, 2H), 1.90 – 1.78 (m, 2H), 1.67 (d, *J* = 8.4 Hz, 2H), 1.40 – 1.18 (m, 4H).

¹³C NMR (100 MHz, DMSO-*d*₆): δ 164.7, 137.8, 123.8, 122.8, 52.1, 50.5, 35.8, 31.1, 24.0.

Anal. Calcd. for C₁₈H₂₈Cl₂N₆O₂: C, 50.12; H, 6.54; N, 19.48. Found: C, 50.20; H, 6.50; N, 19.42.

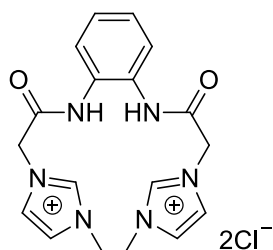
N,N'-(1,2-Phenylene)bis(2-chloroacetamide)



This compound was prepared from benzene-1,2-diamine (2.16 g, 20 mmol) using the method described above. The product was obtained as a solid (4.54 g, 17.4 mmol, 87%), and the characterization data was identical to that reported in the literature.^{S5}

¹H NMR (600 MHz, DMSO-*d*₆): δ 9.81 (s, 2H), 7.56 (dd, *J* = 12.0, 6.0 Hz, 2H), 7.22 (dd, *J* = 12.0, 6.0 Hz, 2H), 4.35 (s, 4H).

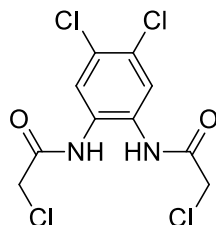
3,3'-((1,2-Phenylenebis(azanediyl))bis(2-oxoethane-2,1-diyl))bis(1-methyl-1H-imidazol-3-ium)



A solution of *N,N'*-(1,2-phenylene)bis(2-chloroacetamide) (6.74 g, 25.8 mmol) and 1-methylimidazole (4.23 g, 51.5 mmol) in acetonitrile was refluxed at 100 °C for 12 h. The mixture was filtered and the solvent was removed under reduced pressure, the product was obtained as a solid (10.75 g, 25.3 mmol, 98%), and the characterization data was identical to that reported in the literature.^{S5}

¹H NMR (600 MHz, DMSO-*d*₆): δ 10.77 (s, 2H), 9.36 (s, 2H), 7.91 (s, 2H), 7.76 (s, 2H), 7.61 (s, 2H), 7.19 (s, 2H), 5.49 (s, 4H), 3.93 (s, 6H).

***N,N'*-(4,5-Dichloro-1,2-phenylene)bis(2-chloroacetamide)**

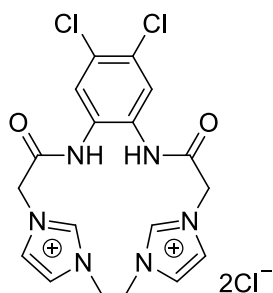


This compound was prepared from 4,5-dichlorobenzene-1,2-diamine (3.54 g, 20 mmol) using the method described above. The product was obtained as a solid powder (2.18 g, 6.6 mmol, 33%).

¹H NMR (600 MHz, DMSO-*d*₆): δ 9.99 (s, 2H), 7.88 (s, 2H), 4.37 (s, 4H).

¹³C NMR (150 MHz, DMSO-*d*₆): δ 165.9, 130.5, 127.4, 126.4, 43.7.

3,3'-(((4,5-Dichloro-1,2-phenylene)bis(azanediyl))bis(2-oxoethane-2,1-diyl))bis(1-methyl-1H-imidazol-3-ium)



A solution of *N,N'*-(4,5-dichloro-1,2-phenylene)bis(2-chloroacetamide) (1.62 g, 4.9 mmol) and 1-methylimidazole (805 mg, 9.8 mmol) in acetonitrile was refluxed at 100 °C for 12 h. The mixture was filtered and the solvent was removed under reduced pressure, the product was obtained as a solid (2.11 g, 4.3 mmol, 87%).

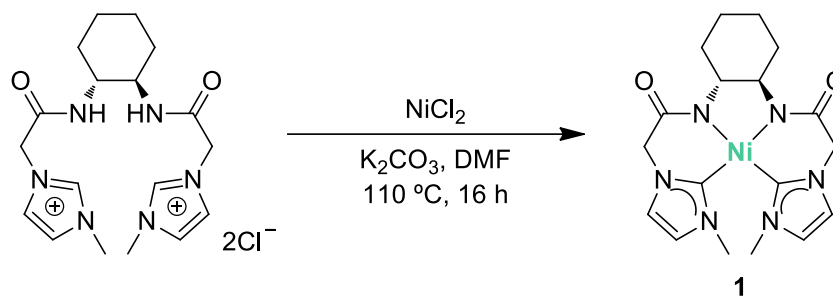
¹H NMR (600 MHz, DMSO-*d*₆): δ 11.13 (s, 2H), 9.32 (s, 2H), 7.94 (s, 2H), 7.88 (s, 2H), 7.76 (s, 2H), 5.47 (s, 4H), 3.93 (s, 6H).

¹³C NMR (150 MHz, DMSO-*d*₆): δ

164.8, 138.1, 137.7, 129.7, 126.5, 125.5, 125.3, 123.9, 123.8, 123.1, 51.5, 35.9.

Anal. Calcd. for $C_{18}H_{20}Cl_4N_6O_2$: C, 43.75; H, 4.08; N, 17.01. Found: C, 43.71; H, 4.14; N, 16.95.

Synthesis and Characterization of Nickel(II) Complexes

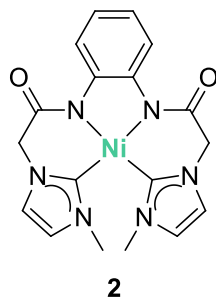


Complex 1: To a solution of 3,3'-(((1*R*,2*R*)-cyclohexane-1,2-diylbis(azanediyl))bis(2-oxoethane-2,1-diyl))bis(1-methyl-1*H*-imidazol-3-ium) (431 mg, 1.0 mmol) and K_2CO_3 (691 mg, 5.0 mmol) in anhydrous *N,N*-dimethylformamide (15 mL), followed by the addition of a solution of NiCl_2 (130 g, 1.0 mmol) in anhydrous *N,N*-dimethylformamide (10 mL). The resultant mixture was refluxed at $110\text{ }^\circ\text{C}$ for 16 h, after that the reaction solution was cooled down to room temperature, the mixture was filtered and the solvent was removed under reduced pressure. Single crystals suitable for X-ray crystallographic analysis were obtained by slow diffusion of anhydrous diethyl ether into a *N,N*-dimethylformamide solution of complex 1 (308 mg, 0.74 mmol, 74%). CCDC 2366466 contains the supplementary crystallographic data for this paper. The data can be obtained free of charge from The Cambridge Crystallographic Data Centre via www.ccdc.cam.ac.uk/structures.

^1H NMR (400 MHz, $\text{DMSO-}d_6$): δ 7.31 – 7.23 (m, 4H), 4.71 (d, $J = 17.6$ Hz, 2H), 4.48 (d, $J = 17.6$ Hz, 2H), 3.12 (s, 6H), 3.07 (d, $J = 7.3$ Hz, 2H), 2.79 (d, $J = 11.4$ Hz, 2H), 1.55 – 1.45 (m, 2H), 1.24 – 1.14 (m, 2H), 0.73 – 0.59 (m, 2H).

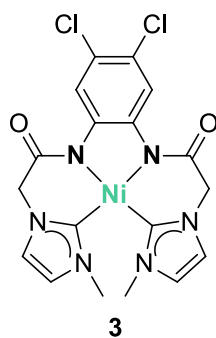
^{13}C NMR (101 MHz, $\text{DMSO-}d_6$) δ 169.7, 163.3, 123.7, 120.6, 68.4, 53.2, 36.3, 31.9, 25.6.

Anal. Calcd. for $\text{C}_{18}\text{H}_{26}\text{N}_6\text{NiO}_2 \cdot \text{DMF}$: C, 51.45; H, 6.79; N, 20.00. Found: C, 51.39; H, 6.75; N, 20.05.



Complex 2: Following the general procedure for the preparation of complex **1** using the ligand of 3,3'-((1,2-phenylenebis(azanediyl))bis(2-oxoethane-2,1-diyl))bis(1-methyl-1H-imidazol-3-ium), provided the title complex as a pale yellow solid (325 mg, 0.79 mmol, 79% yield). The characterization data was identical to that reported in the literature.^{S5}

¹H NMR (600 MHz, DMSO-*d*₆): δ 8.32 (dd, *J* = 6.0, 3.6 Hz, 2H), 7.43 (d, *J* = 1.8 Hz, 2H), 7.33 (d, *J* = 1.8 Hz, 2H), 6.66 (dd, *J* = 6.0, 3.6 Hz, 2H), 5.14 (d, *J* = 16.8 Hz, 2H), 4.68 (d, *J* = 11.4 Hz, 2H), 3.18 (s, 6H).



Complex 3: Following the general procedure for the preparation of complex **1** using the ligand of 3,3'-(((4,5-dichloro-1,2-phenylene)bis(azanediyl))bis(2-oxoethane-2,1-diyl))bis(1-methyl-1H-imidazol-3-ium), provided the title complex as a clear light yellow solid (403 mg, 0.84 mmol, 84% yield). Single crystals suitable for X-ray crystallographic analysis were obtained by slow diffusion of anhydrous diethyl ether into a *N,N*-dimethylformamide solution of complex **3**. CCDC 2366467 contains the supplementary crystallographic data for this paper. The data can be obtained free of charge from The Cambridge Crystallographic Data Centre via www.ccdc.cam.ac.uk/structures.

¹H NMR (400 MHz, DMSO-*d*₆): δ 8.64 (s, 2H), 7.46 (d, *J* = 1.9 Hz, 2H), 7.35 (d, *J* = 1.9 Hz, 2H), 5.24 (d, *J* = 17.0 Hz, 2H), 4.70 (d, *J* = 17.1 Hz, 2H), 3.19 (s, 6H).

^{13}C NMR (101 MHz, DMSO- d_6) δ 167.4, 161.2, 143.7, 123.9, 121.5, 121.3, 120.8, 54.5, 36.2.

Anal. Calcd. for $\text{C}_{18}\text{H}_{18}\text{Cl}_2\text{N}_6\text{NiO}_2 \cdot \text{DMF}$: C, 45.60; H, 4.56; N, 17.73. Found: C, 45.55; H, 4.61; N, 17.88.

References

- (S1) V. Fourmond, P.-A. Jacques, M. Fontecave and V. Artero, *Inorg. Chem.*, 2010, **49**, 10338–10347.
- (S2) H. M. Shahadat, H. A. Younus, N. Ahmad, M. A. Rahaman, Z. A. K. Khattak, S. Zhuiykov and F. Verpoort, *Catal. Sci. Technol.*, 2019, **9**, 5651–5659.
- (S3) S. E. Treimer and D. H. Evans, *J. Electroanal. Chem.*, 1998, **455**, 19–28.
- (S4) P. D. Beer, N. G. Berry, A. R. Cowley, E. J. Hayes, E. C. Oates and W. W. H. Wong, *Chem. Comm.*, 2003, 2408–2409.
- (S5) K. V. Tan, J. L. Dutton, B. W. Skelton, D. J. D. Wilson and P. J. Barnard, *Organometallics*, 2013, **32**, 1913–1923.
- (S6) S. Luo, M. A. Siegler and E. Bouwman, *Eur. J. Inorg. Chem.*, 2016, **2016**, 4693–4700.
- (S7) S. Luo, M. A. Siegler and E. Bouwman, *Eur. J. Inorg. Chem.*, 2019, **2019**, 617–627.
- (S8) K. N. Brinda, Z. Yhobu, J. G. Małeckki, R. S. Keri, R. G. Balakrishna, D. H. Nagaraju and S. Budagumpi, *Int. J. Hydrogen Energy*, 2023, **48**, 10911–10921.
- (S9) A. L. Ostericher, K. M. Waldie and C. P. Kubiak, *ACS Catal.*, 2018, **8**, 9596–9603.
- (S10) S. Xue, X. Lv, N. Liu, Q. Zhang, H. Lei, R. Cao and F. Qiu, *Inorg. Chem.*, 2023, **62**, 1679–1685.
- (S11) Z.-Y. Wu, T. Wang, Y.-S. Meng, Y. Rao, B.-W. Wang, J. Zheng, S. Gao and J.-L. Zhang, *Chem. Sci.*, 2017, **8**, 5953–5961.
- (S12) F. Kamatsos, M. Drosou and C. A. Mitsopoulou, *Int. J. Hydrog. Energy*, 2021, **46**, 19705–19716.
- (S13) A. D. Wilson, R. K. Shoemaker, A. Miedaner, J. T. Muckerman, D. L. Dubois and M. R. Dubois, *Proc. Natl. Acad. Sci. U.S.A.*, 2007, **104**, 6951–6956.
- (S14) S. Norouziyanlakvan, G. K. Rao, J. Ovens, B. Gabidullin and D. Richeson, *Chem. Eur. J.*, 2021, **27**, 13518–13522.
- (S15) C. Hu, R. J. Chew, H. M. Tang, S. Madrahimov, A. A. Bengali and W. Y. Fan, *Mol. Catal.*, 2020, **490**, 110950.

Table S1. Selected Bond Lengths (Å) and Deviation from Planarity (Å) for **1** – **3**

	1 (CCDC 2366466)	2 ^a	3 (CCDC 2366467)
Ni–N _{amide}	1.915(2)	1.917(2)	1.908(2)
	1.904(2)	1.906(2)	1.904(2)
Ni–C _{carbene}	1.852(3)	1.857(3)	1.848(2)
	1.857(3)	1.851(3)	1.849(2)
deviation from planarity ^b	0.5334	0.5117	0.4723
	0.5377	0.5106	0.5182
τ_4	0.2386	0.2286	0.2208

^aTaken from Ref. S5. ^bDistance between the carbene carbon atoms (C1 and C2) and the plane defined by N1, N2, and Ni1.

Table S2. Crystal / Refinement data for **1 – 3**

	1 (CCDC 2366466)	2^a	3 (CCDC 2366467)
Empirical formula	3(C ₁₈ H ₂₄ N ₆ NiO ₂)·2(C ₃ H ₇ NO)	C ₃₇ H ₄₀ N ₁₂ O ₅ Ni ₂	C ₁₈ H ₁₆ Cl ₂ N ₆ NiO ₂ ·2(C ₃ H ₇ NO)
Formula weight	1391.61	850.23	624.17
Temperature / K	293	173	293
Crystal system	Monoclinic	Tetragonal	Monoclinic
Space group	<i>I</i> 2	P4 ₃ 2 ₁ 2	<i>P</i> 2 ₁ / <i>c</i>
<i>a</i> / Å	11.4069(2)	11.3453(16)	15.0789(4)
<i>b</i> / Å	11.1844(2)	11.3453(16)	10.4388(3)
<i>c</i> / Å	27.0255(6)	27.492(6)	17.9250(5)
α / °	90	90	90
β / °	91.7110(17)	90	99.317(3)
γ / °	90	90	90
Volume / Å ³	3446.36(12)	3538.7(10)	2784.27(14)
<i>Z</i>	2	4	4
ρ_{calc} mg/mm ³	1.341	1.596	1.489
μ /mm ⁻¹	0.877	1.129	0.935
F(000)	1468	1768	1296
Crystal size /mm ³	0.025 × 0.024 × 0.023	0.2 × 0.2 × 0.1	0.50 × 0.40 × 0.40
Wavelength / Å	Mo <i>K</i> α , 0.71073	Mo <i>K</i> α , 0.71073	Mo <i>K</i> α , 0.71073
2 θ range for data collection	3.9 to 28.8°	5.08 to 51.36°	3.8 to 28.4°
Index ranges	-14 ≤ <i>h</i> ≤ 14 -13 ≤ <i>k</i> ≤ 13 -33 ≤ <i>l</i> ≤ 33	-10 ≤ <i>h</i> ≤ 13 -10 ≤ <i>k</i> ≤ 11 -20 ≤ <i>l</i> ≤ 33	-18 ≤ <i>h</i> ≤ 19 -14 ≤ <i>k</i> ≤ 13 -22 ≤ <i>l</i> ≤ 22
Reflections	27789	8850	18576
Independent	7020 [<i>R</i> (int) = 0.0242]	3361 [<i>R</i> (int) =	6494 [<i>R</i> (int) = 0.0292]
Data/restraints/parameters	7020/1/416	3361/0/266	6494/0/358
Goodness-of-fit on <i>F</i> ²	1.062	1.083	1.033
Final <i>R</i> indexes [<i>I</i> > 2 σ (<i>I</i>)]	<i>R</i> ₁ = 0.0260, <i>wR</i> ₂ = 0.0622	<i>R</i> ₁ = 0.0296, <i>wR</i> ₂ = 0.0723	<i>R</i> ₁ = 0.0380, <i>wR</i> ₂ = 0.0844
Final <i>R</i> indexes [all data]	<i>R</i> ₁ = 0.0303, <i>wR</i> ₂ = 0.0649	<i>R</i> ₁ = 0.0324, <i>wR</i> ₂ = 0.0738	<i>R</i> ₁ = 0.0583, <i>wR</i> ₂ = 0.0939
Largest diff. peak/hole/e Å ⁻³	0.267/-0.185	0.28/-0.34	0.324/-0.277

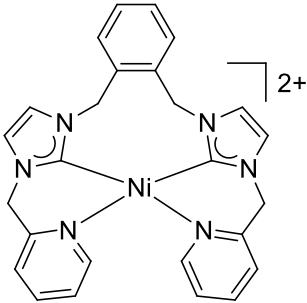
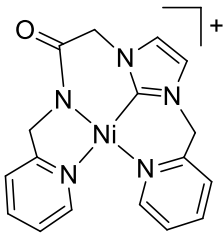
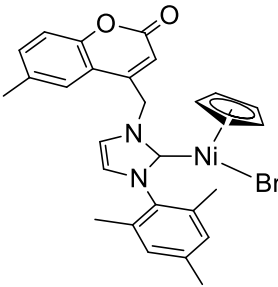
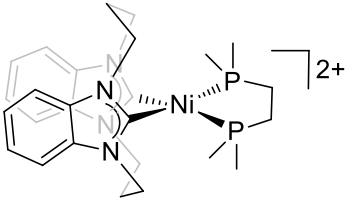
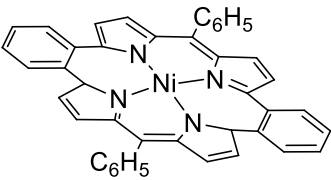
^aTaken from Ref. S5

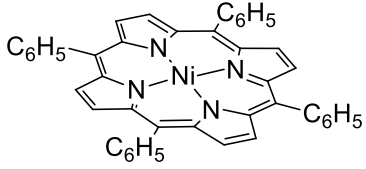
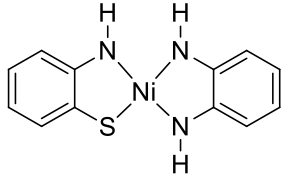
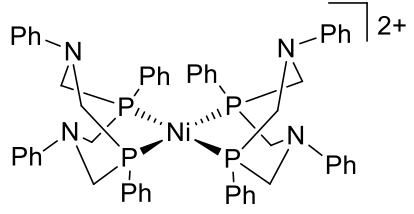
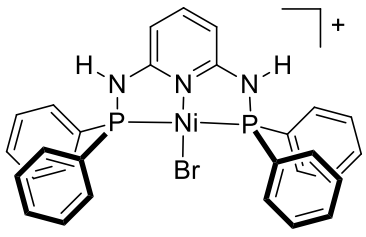
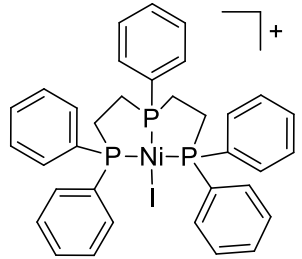
Table S3. Selected Bond Distances (Å) and Angles (°) for **1** – **3**

Identification code	1 (CCDC 2366466)	2 ^a	3 (CCDC 2366467)
Bond Distances (Å)			
Ni1-N1	1.904(2)	1.917(2)	1.9041(16)
Ni1-N2	1.915(2)	1.906(2)	1.9084(16)
Ni1-C1	1.852(3)	1.857(3)	1.849(2)
Ni1-C2	1.857(3)	1.851(3)	1.848(2)
Bond Angles (°)			
N1-Ni1-N2	87.32(11)	86.01(9)	86.21(7)
N1-Ni1-C1	91.73(11)	93.24(10)	92.40(8)
N2-Ni1-C2	91.21(12)	91.08(12)	92.96(8)
C1-Ni1-C2	94.42(12)	93.89(13)	92.46(9)
N1-Ni1-C2	163.13(12)	163.74(11)	163.69(8)
N2-Ni1-N3	163.23(12)	164.02(11)	165.16(8)

^aTaken from Ref. S5

Table S4. Comparison of the Electrocatalytic HER Performance of the Nickel Complex Described in This Work with the Reported Ones

Cat.	Overpotential (mV)	Proton source	Potential ^a	Faraday efficiency	TOF (s ⁻¹)	Ref.
1	780	CF ₃ CO ₂ H in CH ₃ CN	-1.60 V vs Fc/Fc ⁺	45%	316	this work
2	770	CF ₃ CO ₂ H in CH ₃ CN	-1.60 V vs Fc/Fc ⁺	54%	409	this work
3	760	CF ₃ CO ₂ H in CH ₃ CN	-1.60 V vs Fc/Fc ⁺	64%	698	this work
	1280	CH ₃ CO ₂ H in DMF	-	-	490	S6
	860	CH ₃ CO ₂ H in DMF	-1.80 V vs Fc/Fc ⁺	85%	240	S7
	347	0.5 M H ₂ SO ₄	-	-	-	S8
	400	C ₆ H ₅ OH in CH ₃ CN	-1.90 V vs Fc/Fc ⁺	-	1000	S9
	330	CF ₃ CO ₂ H in CH ₃ CN	-1.65 V vs Fc/Fc ⁺	94%	175	S10

	930	CF ₃ CO ₂ H in CH ₃ CN	-	> 90%	6287	S11
	910	CF ₃ CO ₂ H in DMF	-	-	46	S12
	-	H ⁺ -DMF(OTf)/DMF in CH ₃ CN	-	-	350	S13
	-	H ₂ O in CH ₃ CN	-2.55 V vs Fc/Fc ⁺	87%	160	S14
	700	CF ₃ CO ₂ H in CH ₃ CN	-2.50 V vs Fc/Fc ⁺	37%	-	S15

^aPotentials is the controlled potential electrolysis (CPE).

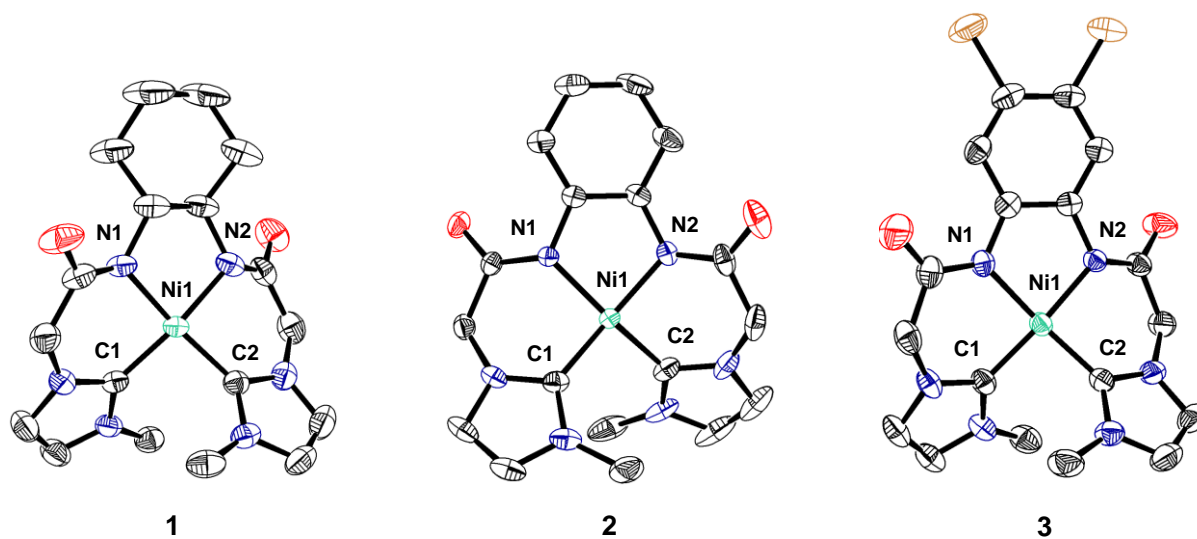


Fig. S1. X-ray crystal structures of **1** – **3** as an ORTEP drawing with 50% probability ellipsoids (Ni, medium aquamarine; N, new midnight blue; O, red; Cl, gold; C, black).

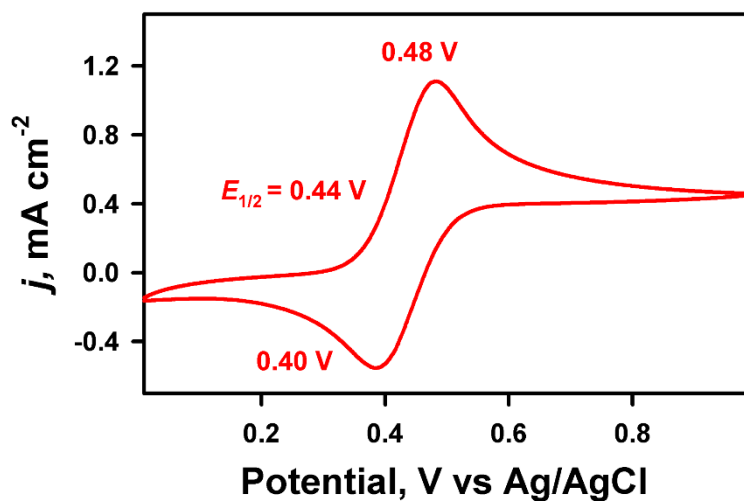


Fig. S2. CV of 1.0 mM ferrocene in deaerated CH₃CN. Conditions: 0.1 M *n*-Bu₄NPF₆, GC working electrode, 100 mV s⁻¹ scan rate, 25 °C.

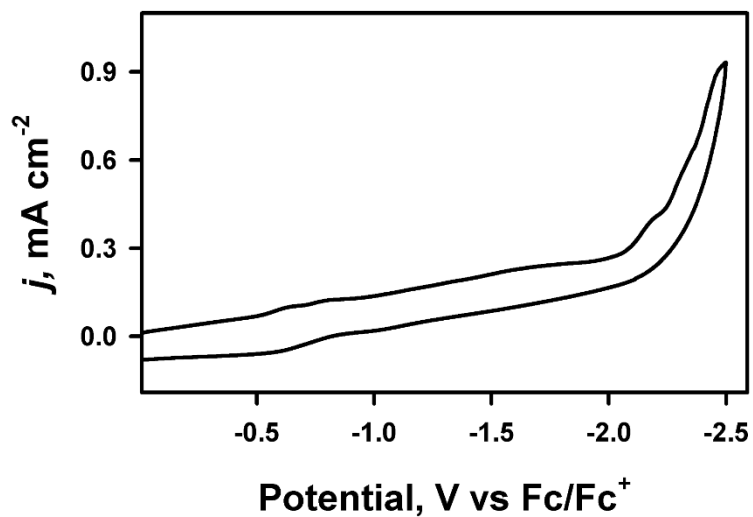


Fig. S3. CV of 1.0 mM L1 in deaerated CH₃CN. Conditions: 0.1 M *n*-Bu₄NPF₆, GC working electrode, 100 mV s⁻¹ scan rate, 25 °C.

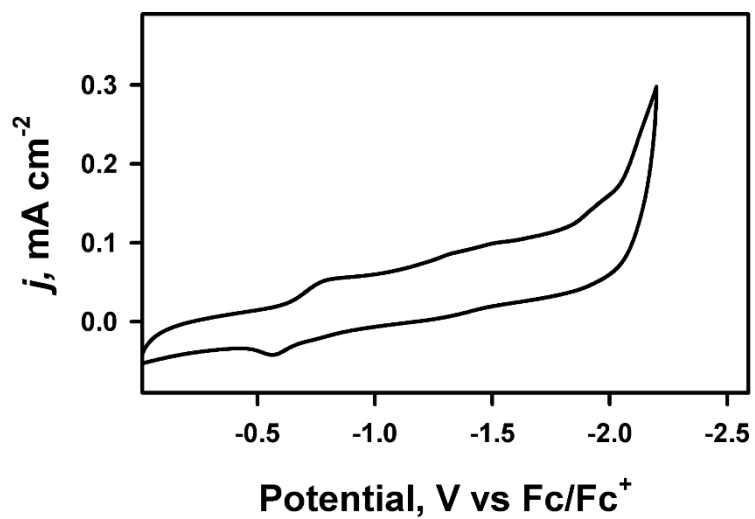


Fig. S4. CV of 1.0 mM **L2** in deaerated CH₃CN. Conditions: 0.1 M *n*-Bu₄NPF₆, GC working electrode, 100 mV s⁻¹ scan rate, 25 °C.

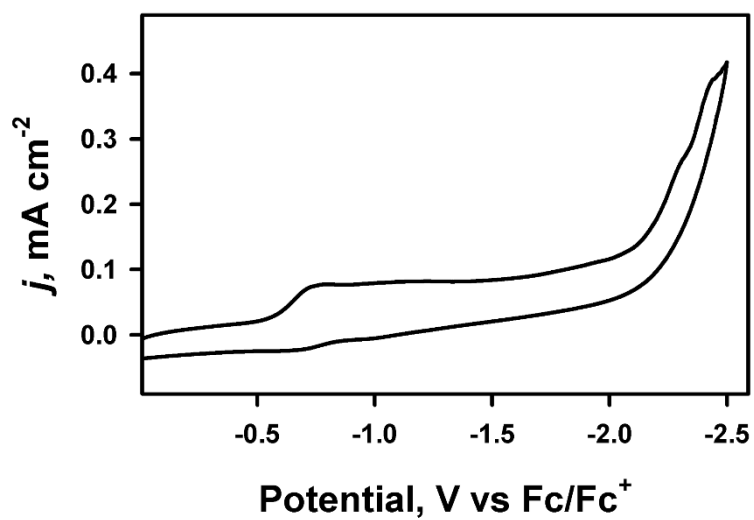


Fig. S5. CV of 1.0 mM **L3** in deaerated CH_3CN . Conditions: 0.1 M $n\text{-Bu}_4\text{NPF}_6$, GC working electrode, 100 mV s^{-1} scan rate, $25 \text{ }^\circ\text{C}$.

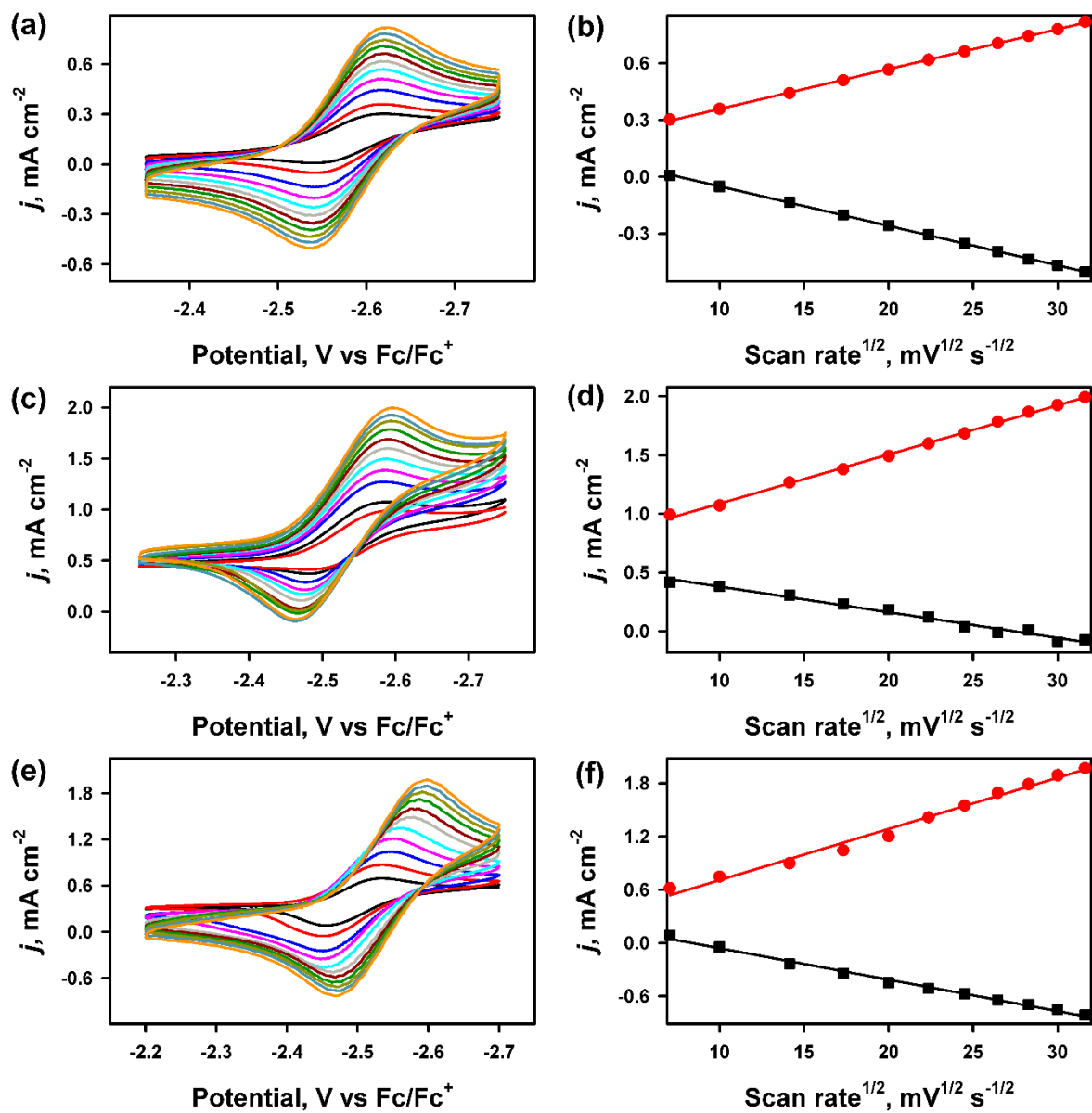


Fig. S6. CVs of 1 mM **1** (a), **2** (c) and **3** (e) in deaerated CH₃CN at various scan rates (50 mV s⁻¹ to 1000 mV s⁻¹) and corresponding Randles–Sevcik analysis (b, d, f). Conditions: 0.1 M *n*-Bu₄NPF₆, GC working electrode, 25 °C.

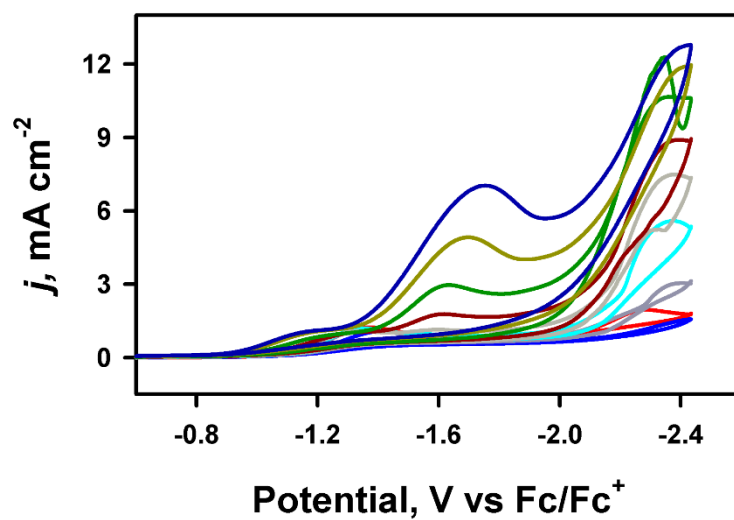


Fig. S7. CVs of increasing TFA concentration in the absence of nickel complex in deaerated CH₃CN. Conditions: 0.1 M *n*-Bu₄NPF₆, GC working electrode, 100 mV s⁻¹ scan rate, 25 °C.

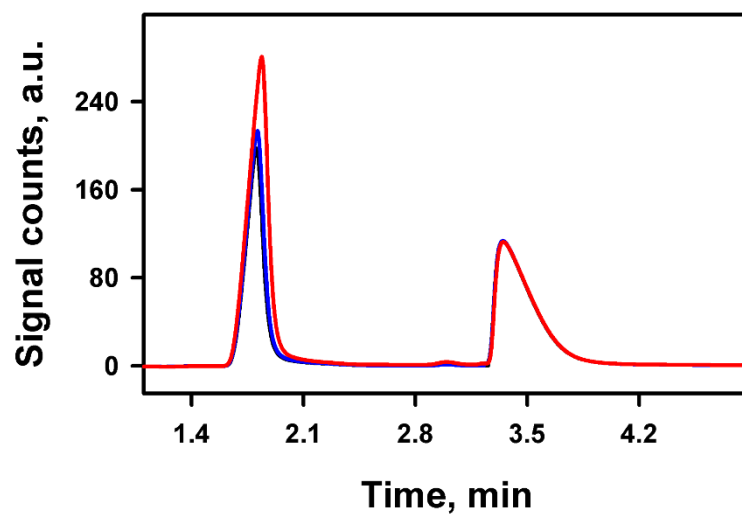
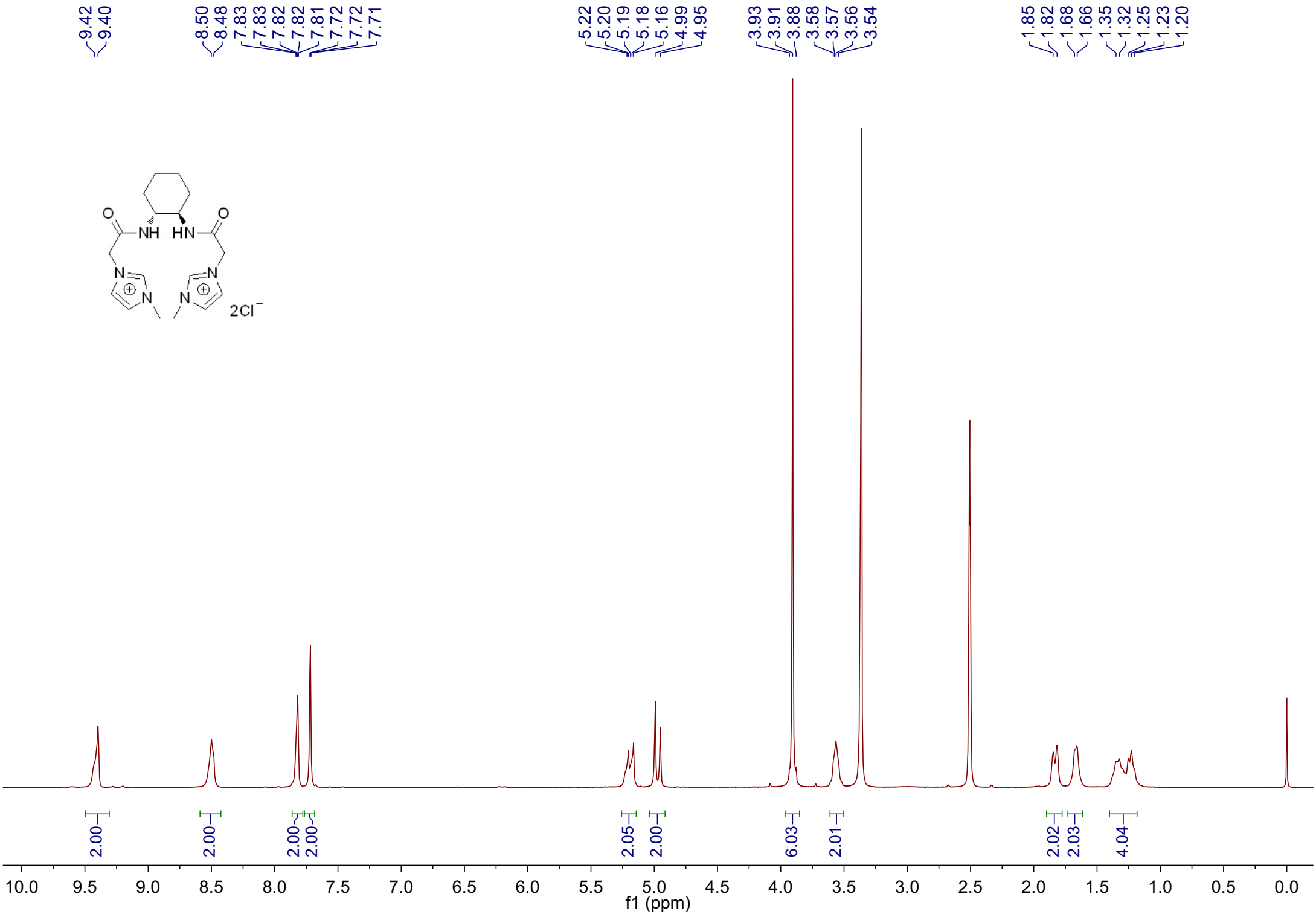
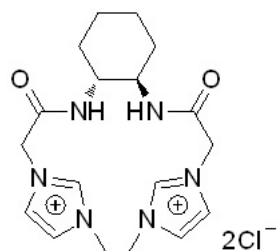


Fig. S8. GC plot of the gas collected from the headspace during the CPE experiment of complex **1** (black line), **2** (blue line), and **3** (red line).

Additional Data: ^1H and ^{13}C NMR spectra





—164.7

—137.8

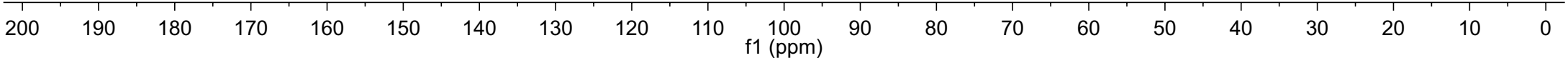
~123.8
~122.8

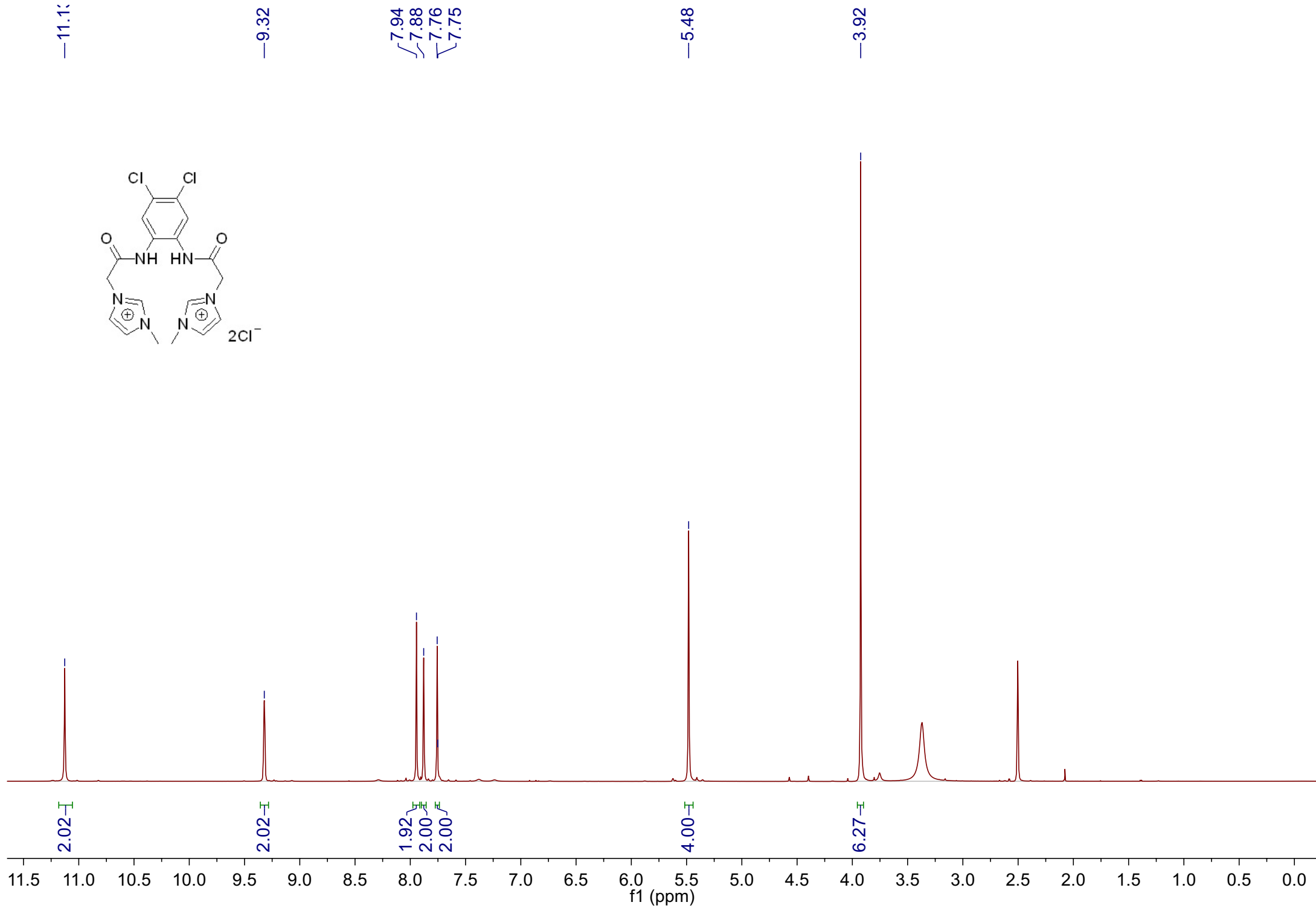
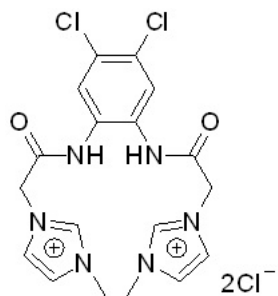
~52.1
~50.5

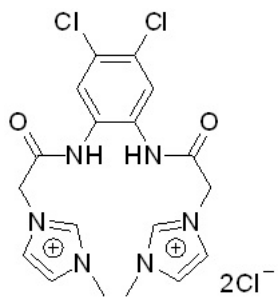
—35.8

—31.1

—24.0





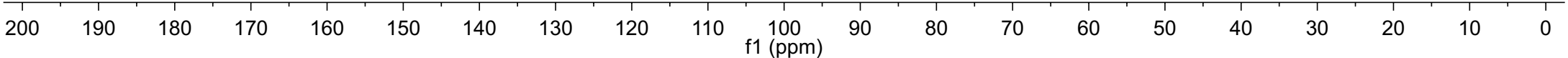


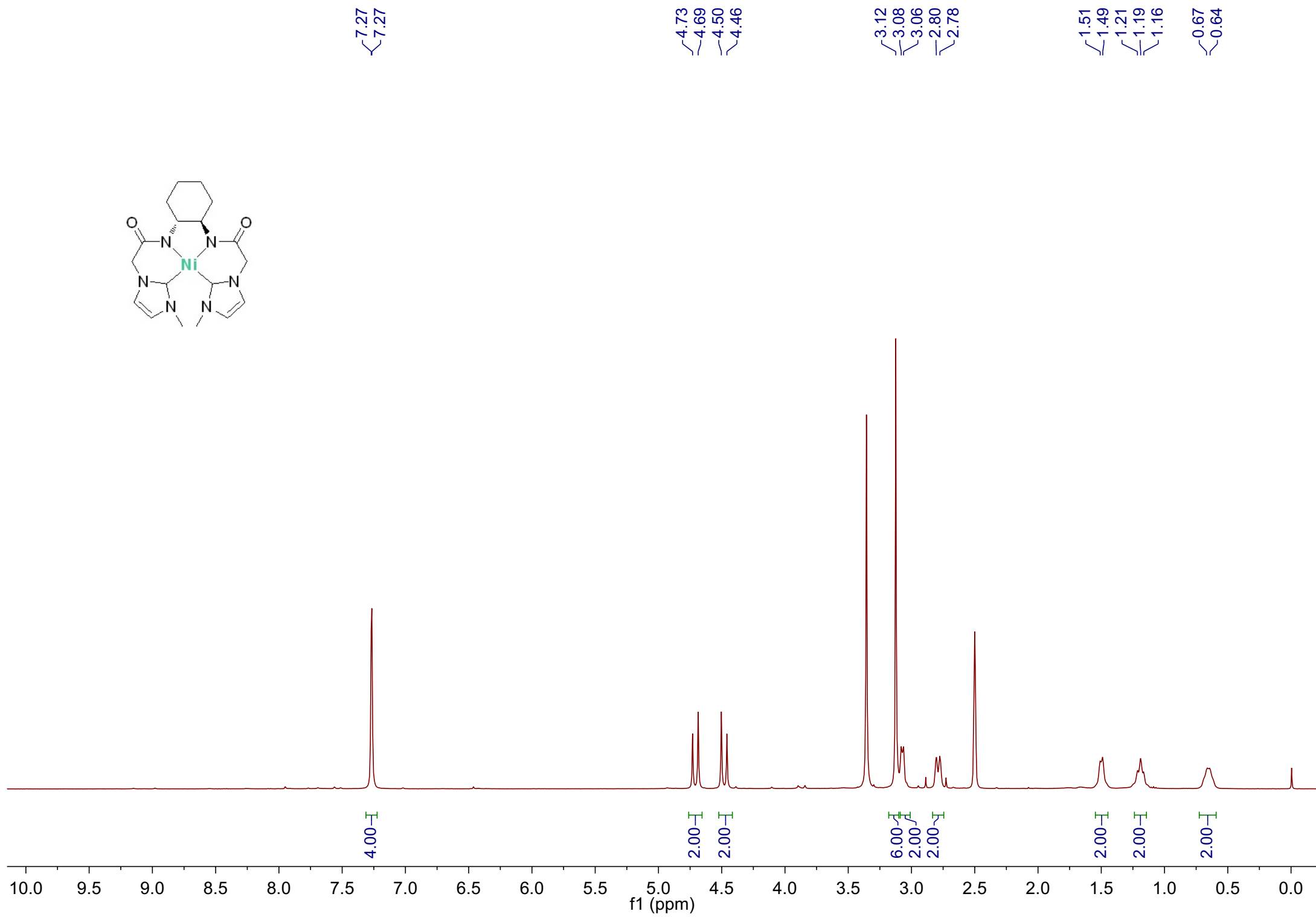
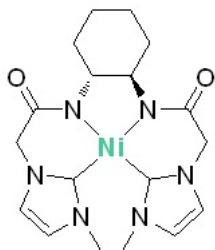
—164.8

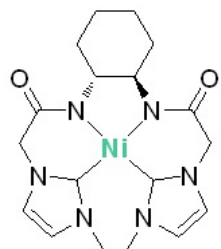
138.1
137.7
129.7
126.5
125.5
125.3
123.9
123.8
123.1

—51.5

—35.9







—169.7

—163.3

—123.7

—120.6

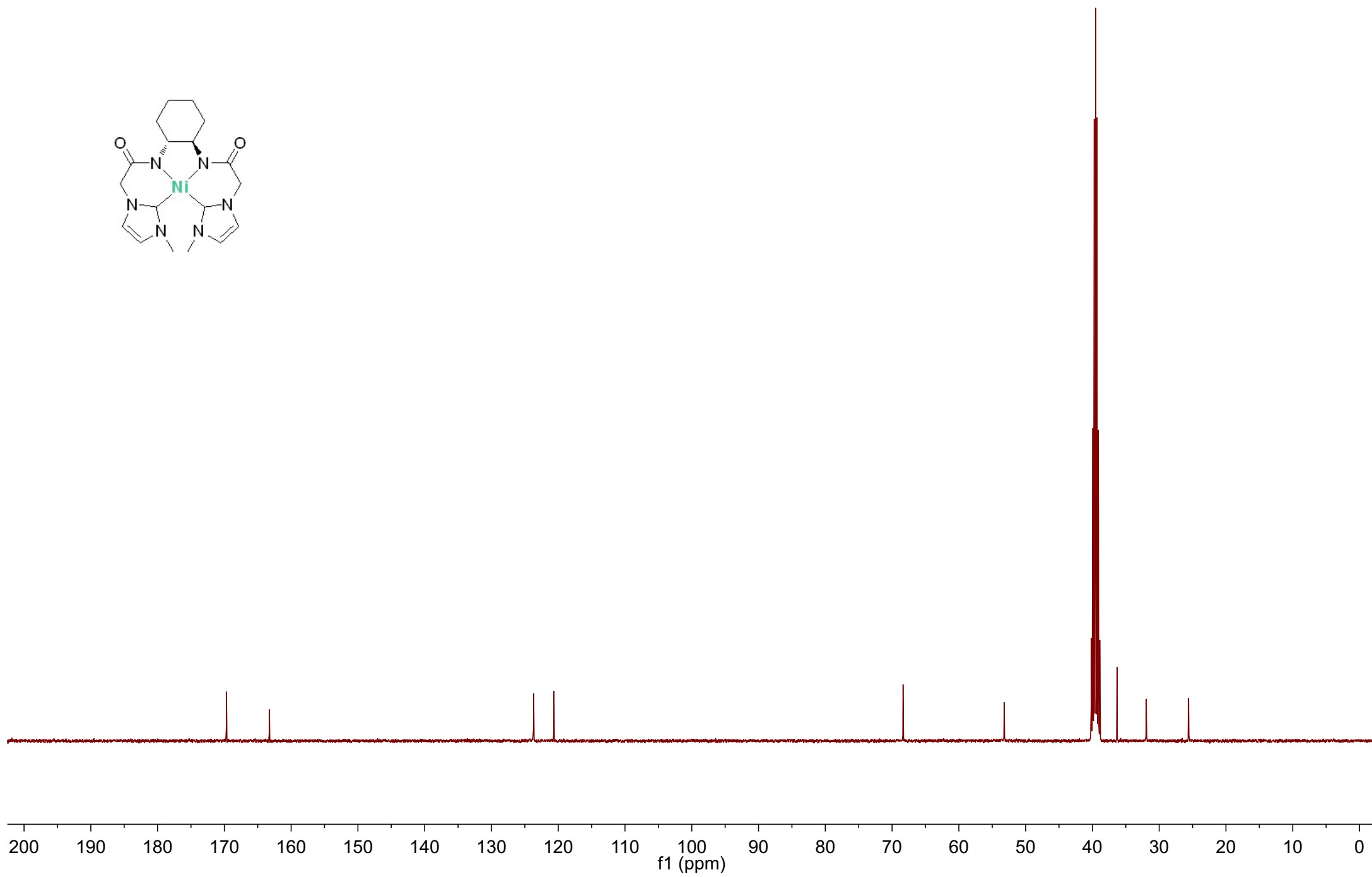
—68.4

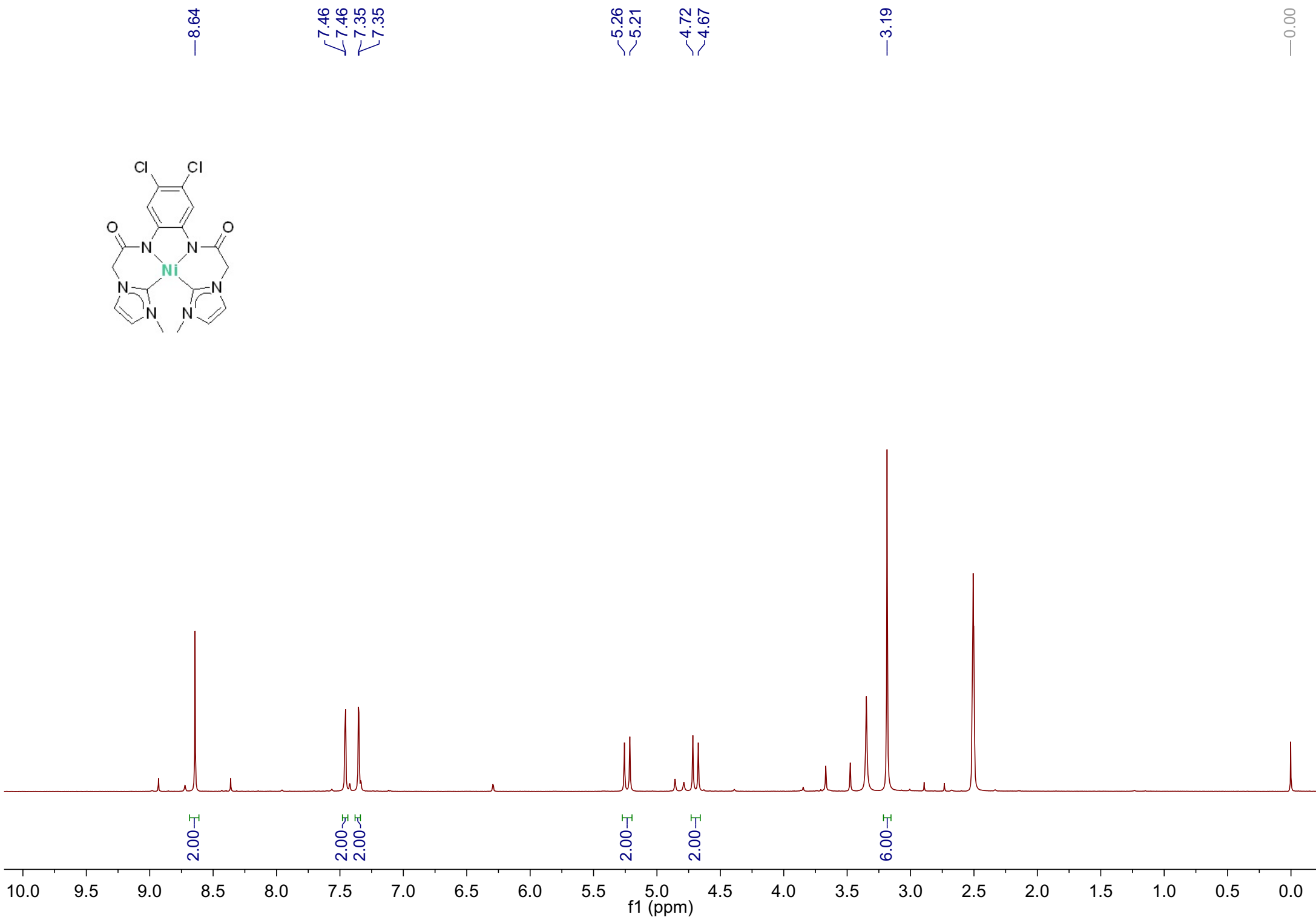
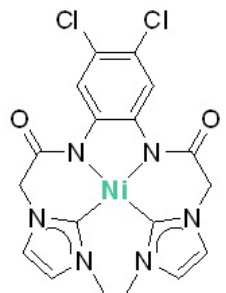
—53.2

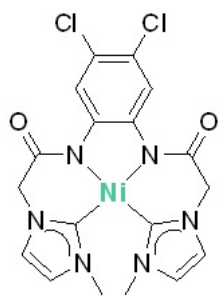
—36.3

—31.9

—25.6







—167.4

—161.2

—143.7

—123.9

—121.5

—121.3

—120.8

—54.5

—36.2

